INTERNATIONAL JOURNAL FOR NUMERICAL METHODS IN FLUIDS
Int. J. Numer. Meth. Fluids 2011; **65**:1084–1095
Published online 5 February 2010 in Wiley Online Library (wileyonlinelibrary.com). DOI: 10.1002/fld.2230

Axisymmetric stagnation flow obliquely impinging on a moving circular cylinder with uniform transpiration

Asghar B. Rahimi and M. Esmaeilpour*, †

Faculty of Engineering, Ferdowsi University of Mashhad, P.O. Box No. 91775-1111, Mashhad, Iran

SUMMARY

Laminar stagnation flow, axisymmetrically yet obliquely impinging on a moving circular cylinder, is formulated as an exact solution of the Navier–Stokes equations. Axial velocity is time-dependent, whereas the surface transpiration is uniform and steady. The impinging free stream is steady with a strain rate $\bar{k}$. The governing parameters are the stagnation-flow Reynolds number $Re = \bar{k}a^2/2\nu$, and the dimensionless transpiration $S = U_0/\bar{k}a$. An exact solution is obtained by reducing the Navier–Stokes equations to a system of differential equations governed by Reynolds number and the dimensionless wall transpiration rate, S. The system of Boundary Value Problems is then solved by the shooting method and by deploying a finite difference scheme as a semi-similar solution. The results are presented for velocity similarity functions, axial shear stress and stream functions for a variety of cases. Shear stresses in all cases increase with the increase in Reynolds number and suction rate. The effect of different parameters on the deflection of viscous stagnation circle is also determined. Copyright © 2010 John Wiley & Sons, Ltd.

Received 26 May 2009; Revised 2 September 2009; Accepted 16 October 2009

KEY WORDS: oblique stagnation-point flow; axisymmetric; transpiration; exact solution

1. INTRODUCTION

The task of finding exact solutions for the Navier–Stokes equations is a difficult one due to nonlinearity of these equations. Hiemenz [1] has obtained an exact solution of the Navier–Stokes equations governing the two-dimensional stagnation-point flow on a flat plate. Homann [2] investigated the analogous axisymmetrtic stagnation-point flow. Howarth [3] and Davey [4] presented results of the problem of stagnation flow against a flat plate for asymmetric cases. Wang [5] was the first to find an exact solution for the problem of axisymmetric stagnation flow on infinite stationary circular cylinder. Gorla [6–10], in a series of papers, studied the steady and unsteady flows and heat transfer over a circular cylinder in the vicinity of the stagnation point for the cases of constant axial movement, and the special case of axial harmonic motion of a non-rotating cylinder. This special case is only for small and high values of the frequency parameters using perturbation techniques. Cunning *et al.* [11] considered the stagnation flow problem on a rotating circular cylinder with constant angular velocity, including the effects of suction and blowing with constant rate. Takhar *et al.* [12] also investigated the unsteady viscous flow near an axisymmetric stagnation point of an infinite circular cylinder when both the cylinder and the free-stream velocities vary as a same function of time. Their self-similar solution is only for the case when both the cylinder and the free-stream velocities vary inversely as a linear function of time and by taking an average value for

*Correspondence to: M. Esmaeilpour, Faculty of Engineering, Ferdowsi University of Mashhad, P.O. Box No. 91775-1111, Mashhad, Iran.
†E-mail: Esmaeilpour.mehdi@gmail.com

the Reynolds number. Recently, axisymmetric stagnation point flow and heat transfer of a viscous fluid on a circular cylinder with time-dependent axial velocity has been considered by Saleh and Rahimi [13] and for the rotating cylinder with time-dependent angular velocity has been done by Rahimi and Saleh [14]. Also, the case of unaxisymmetric heat transfer in stagnation-point flow on a cylinder with simultaneous axial and rotational movements has been studied by Rahimi and Saleh [15]. Aside from many stagnation-point flow problem studies of micropolar type in the literature, the study by Ziabakhsh *et al.* [16] which is in a porous medium and used in the homotopy analysis method can be mentioned.

In the present analysis, the unsteady viscous flow in the vicinity of an axisymmetric stagnation point of an infinite cylinder with time-dependent axial movement and with uniform and steady normal transpiration U_0 is investigated when the flow is oblique. This obliquely impinging free stream is composed of an axial shear flow superposed onto a radial stagnation flow normal to the cylinder. The relative importance of these two flows is measured by a parameter γ. In other words, γ is the ratio of the strength of outer axial shear flow to the strength of outer radial flow. An exact solution is obtained by reduction of the Navier–Stokes equations to a system of differential equations using appropriate semi-similar coordinate separations. The semi-similar equations are turned into a system of ordinary differential equations using separation of variables. The system of BVPs is then solved by the shooting method for limited cases of boundary conditions. In order to analyze all the possible boundary conditions, namely general cases of and axial movement, semi-similar equations are solved directly by deploying a finite difference scheme as a semi-similar solution. The results are presented for velocity similarity functions in terms of different values of Reynolds number, $Re=\bar{k}a^2/2v$ and for different values of dimensionless transpiration rate, $S=U_0/\bar{k}a$, where a is the cylinder radius and v is the fluid kinematic viscosity. Axial shear stress at different Reynolds numbers is presented for different forms of cylinder movements and selected values of uniform suction and blowing rates. The stream surfaces are shown and the deflection of the stagnation circle from its assumed location is calculated.

2. PROBLEM FORMULATION

Flow is considered in cylindrical coordinates (r, φ and z) with corresponding velocity components (U, V, W) for outer flow and (u, v, w) for the viscous flow. A model of the flow with the coordinate system is shown in Figure 1. We consider the laminar unsteady incompressible flow of a viscous flow in the neighborhood of an axisymmetric stagnation point of an infinite circular cylinder when the axial velocity of the cylinder varies as specified time-dependent functions while the cylinder has surface transpiration.

An external axisymmetric radial stagnation flow of strength $\bar{k}$ impinges on the cylinder of radius a, centered at $r=0$. The location of the stagnation circle of the inviscid outer flow is

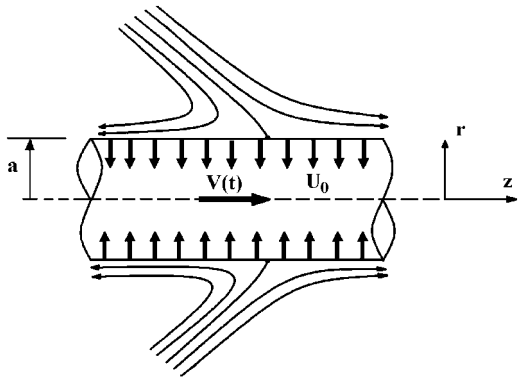

Figure 1. Schematic of an oblique stagnation flow.

DOI: 10.1002/fld

at $z=0$. A uniform and steady normal transpiration U_0 may occur at cylinder surface, where $U_0>0$ corresponds to suction into the cylinder and $U_0<0$ corresponds to blowing out of it.

The outer flow stream function has been defined in References [11, 17] as follows:

$$\psi=\bar{k}(r^2-a^2)z+\frac{\gamma\bar{k}}{8a}(r^2-a^2)^2+aU_0z. \tag{1}$$

Therefore, the free-stream velocities are:

$$U=-\bar{k}\left(r-\frac{a^2}{r}\right)-U_0\frac{a}{r}, \tag{2}$$

$$W=2\bar{k}z+\frac{\gamma}{2}\bar{k}a\left(\frac{r^2}{a^2}-1\right). \tag{3}$$

The unsteady Navier–Stokes equations in cylindrical polar coordinates governing the axisymmetric flow are given by [5–10]:

Mass:

$$\frac{\partial u}{\partial r}+\frac{u}{r}+\frac{\partial w}{\partial z}=0. \tag{4}$$

Momentum:

$$\frac{\partial u}{\partial t}+u\frac{\partial u}{\partial r}+w\frac{\partial u}{\partial z}=-\frac{1}{\rho}\frac{\partial p}{\partial r}+\nu\left(\frac{\partial^2 u}{\partial r^2}+\frac{1}{r}\frac{\partial u}{\partial r}-\frac{u}{r^2}+\frac{\partial^2 u}{\partial z^2}\right), \tag{5}$$

$$\frac{\partial w}{\partial t}+u\frac{\partial w}{\partial r}+w\frac{\partial w}{\partial z}=-\frac{1}{\rho}\frac{\partial p}{\partial z}+\nu\left(\frac{\partial^2 w}{\partial r^2}+\frac{1}{r}\frac{\partial w}{\partial r}+\frac{\partial^2 w}{\partial z^2}\right), \tag{6}$$

where p, ρ and ν are the fluid pressure, density and kinematic viscosity, respectively. The boundary conditions are:

$$r=a: u=-U_0, \quad w=V(t), \tag{7}$$

$$r\to\infty: u=-\bar{k}\left(r-\frac{a^2}{r}\right)-U_0\frac{a}{r}, \quad w=2\bar{k}z+\frac{\gamma}{2}\bar{k}a(\eta-1). \tag{8}$$

These boundary conditions are in fact the relations (2) and (3) but at $r=a$ and at $r\to\infty$, respectively, since the viscous flow solution approaches the potential flow as $r\to\infty$. A reduction of the Navier–Stokes equations is obtained by the following coordinate separation:

$$\eta=\frac{r^2}{a^2}, \tag{9}$$

$$\tau=2\bar{k}t, \tag{10}$$

$$u=-\frac{\bar{k}a}{\sqrt{\eta}}f(\eta), \tag{11}$$

$$w=2\bar{k}zf'(\eta)+\frac{\gamma\bar{k}a}{2}g'(\eta)+\bar{k}aH(\eta,\tau), \tag{12}$$

$$p=\rho a^2\bar{k}^2P(\eta,z,\tau), \tag{13}$$

where η and τ are radial variable and dimensionless time, and prime denotes differentiation with respect to η. These transformations satisfy continuity equation automatically and their insertion

DOI: 10.1002/fld

into (5) and (6) yields a coupled system of differential equations in terms of $f(\eta)$, $g(\eta)$ and $H(\eta,\tau)$, and an expression for the pressure:

$$\eta f''' + f'' + Re(1 + ff'' - f'^2) = 0, \tag{14}$$

$$\eta g''' + g'' + Re(fg'' - f'g') = 0, \tag{15}$$

$$\eta H'' + H' + Re\left(fH' - Hf' - \frac{\partial H}{\partial \tau}\right) = 0, \tag{16}$$

$$p - p_0 = -\frac{f^2}{2\eta} - \frac{1}{Re} f' - 2\left(\frac{z}{a}\right)^2. \tag{17}$$

In these equations prime indicates differentiation with respect to η and $Re = \bar{k}a^2/2v$ is the Reynolds number and P_0 is the stagnation pressure. The boundary conditions for (14), (15) and (16) are as follows:

$$f(1) = S, \quad f'(1) = 0, \quad f'(\infty) = 1 \tag{18}$$

$$g(1) = 0, \quad g'(1) = 0, \quad g''(\infty) = 1 \tag{19}$$

$$H(1,\tau) = v(\tau), \quad H(\infty,\tau) = 0. \tag{20}$$

In which $S = U_0/\bar{k}a$ is the dimensionless wall transpiration rate. Equation (14) is the same as the one obtained by Wang [5] and its solution is known.

3. SELF-SIMILAR EQUATIONS

Equation (16) can be reduced to a system of ordinary differential equation if we assume that the function $H(\eta,\tau)$ in this equation is separable as:

$$H(\eta,\tau) = h(\eta)\cdot v(\tau). \tag{21}$$

Substituting this separation of variables into (16), correspondingly gives:

$$\eta\frac{h''}{h} + \frac{h'}{h} + Re\left(f\frac{h'}{h} - f'\right) = Re\frac{\mathrm{d}v(\tau)/\mathrm{d}\tau}{v(\tau)}. \tag{22}$$

The general solution to the differential equations in (21) and (22) with τ as an independent variable is as the following:

$$v(\tau) = b\cdot \mathrm{Exp}[(\alpha_1 + \mathrm{i}\beta_1)\tau], \tag{23}$$

Here, $\mathrm{i} = \sqrt{-1}$ and b, α_1 and β_1 are constants. Substituting these solutions into the differential equations in (22) with η as independent variable results in:

$$\eta h'' + h' + Re(fh' - hf' - \alpha_1 h - \mathrm{i}\beta_1 h) = 0. \tag{24}$$

The boundary conditions are:

$$\eta = 1: \quad h = 1, \tag{25}$$

$$\eta \to \infty: \quad h = 0. \tag{26}$$

Different combinations of values of b, α and β in (23) give different time-dependent axial movements. In order to obtain solutions of Equations (24), it is assumed that the function $h(\eta)$ is complex function like:

$$h(\eta) = h_1(\eta) + \mathrm{i}h_2(\eta). \tag{27}$$

DOI: 10.1002/fld

Substituting (27) into (24), the following coupled system of differential equations is obtained:

$$\begin{aligned} \eta h_1'' + h_1' + Re(f h_1' - h_1 f' - \alpha_1 h_1 + \beta_1 h_2) = 0, \\ \eta h_2'' + h_2' + Re(f h_2' - h_2 f' - \alpha_1 h_2 - \beta_1 h_1) = 0. \end{aligned} \tag{28}$$

The boundary conditions for the function $h(\eta)$ becomes:

$$\eta = 1: \quad h_1 = 1, \quad h_2 = 0, \tag{29}$$

$$\eta \to \infty: \quad h_1 = 0, \quad h_2 = 0. \tag{30}$$

The coupled system of Equations (28) along with boundary conditions is solved by using a fourth-order Runge–Kutta method of numerical integration along with a shooting method, Press *et al.* [18].

4. SEMI-SIMILAR EQUATIONS

Equation (16) may be solved directly for any chosen $v(\tau)$ function. The solutions obtained in this way are called semi-similar solutions. They have the advantage of predicting the H function at the initial times and also the ability of analyzing all the possible boundary conditions, namely all the $v(\tau)$ functions. This equation along with its corresponding boundary conditions is solved using a Crank-Nicholson scheme. Each solution starts at $\tau = 0$ and marches through time as it satisfies the boundary conditions. The initial values, except for the first node, are all set to zero for this case (Equation (16)), assuming that the cylinder is stationary at $\tau < 0$. The results will be presented for a few selected functions in later sections.

5. APPROXIMATE SOLUTION FOR LARGE RE

In order to deploy the shooting method we need an initial guess. Finding this initial guess is an extremely difficult task for large Reynolds numbers especially when transpiration exists. Thus, in the case of large Re numbers the advantage of finding initial guess compensates the difficulty of solving another system of BVPs. It is desirable to obtain the asymptotic nature of solutions for large values of Re where numerical integration becomes increasingly difficult. The leading term solution of a perturbation expansion can be used as an initial guess. We now proceed by introducing $\varepsilon = 1/\sqrt{Re}$ as the perturbation parameter and in order to magnify this tiny region the following change of variables is made:

$$\xi = \frac{\eta - 1}{\varepsilon}, \tag{31}$$

$$\hat{F}(\xi) = \frac{f(\eta)}{\varepsilon}, \tag{32}$$

$$\hat{G}(\xi) = \frac{g(\eta)}{\varepsilon}, \tag{33}$$

$$\hat{H}(\xi) = h(\eta). \tag{34}$$

Using these change of variables, the boundary value problems (14), (15), and (24) change into:

$$(1 + \varepsilon\xi)\hat{F}''' + \varepsilon\hat{F}'' + \hat{F}\hat{F}'' - \hat{F}'^2 + 1 = 0, \tag{35}$$

$$(1 + \varepsilon\xi)\hat{G}''' + \varepsilon\hat{G}'' + \hat{F}\hat{G}'' - \hat{F}'\hat{G}' = 0, \tag{36}$$

$$(1 + \varepsilon\xi)\hat{H}'' + \varepsilon\hat{H}' + \hat{F}\hat{H}' - \hat{F}'\hat{H} - (\alpha_1 + \mathrm{i}\beta_1)\hat{H} = 0. \tag{37}$$

DOI: 10.1002/fld

The following separation of variables is used:

$$\hat{H}(\xi)=\hat{H}_1(\xi)+\mathrm{i}\hat{H}_2(\xi), \tag{38}$$

The following regular perturbation expansions are assumed:

$$\hat{F}(\xi,\varepsilon)=\hat{F}_0(\xi)+\varepsilon\hat{F}_1(\xi)+o(\varepsilon^2), \tag{39}$$

$$\hat{G}(\xi,\varepsilon)=\hat{G}_0(\xi)+\varepsilon\hat{G}_1(\xi)+o(\varepsilon^2), \tag{40}$$

$$\hat{H}_1(\xi,\varepsilon)=\hat{H}_{1-0}(\xi)+\varepsilon\hat{H}_{1-1}(\xi)+o(\varepsilon^2), \tag{41}$$

$$\hat{H}_2(\xi,\varepsilon)=\hat{H}_{2-0}(\xi)+\varepsilon\hat{H}_{2-1}(\xi)+o(\varepsilon^2). \tag{42}$$

Inserting these expansions into Equations (35)–(37) and collecting all the coefficients of like powers and setting them equal to zero, the following systems are obtained:

$$\varepsilon^0:\begin{cases}\hat{F}_0'''+\hat{F}_0\hat{F}_0''+\hat{F}_0'^2-1=0,\\ \hat{G}_0'''+\hat{F}_0\hat{G}_0''-\hat{F}_0'\hat{G}_0'=0,\\ \hat{H}_{1-0}''+\hat{F}_0\hat{H}_{1-0}'-\hat{F}_0'\hat{H}_{1-0}-\alpha_1\hat{H}_{1-0}+\beta_1\hat{H}_{2-0}=0,\\ \hat{H}_{2-0}''+\hat{F}_0\hat{H}_{2-0}'-\hat{F}_0'\hat{H}_{2-0}-\alpha_1\hat{H}_{2-0}-\beta_1\hat{H}_{1-0}=0.\end{cases} \tag{43}$$

And

$$\varepsilon^1:\begin{cases}\hat{F}_1'''+\xi\hat{F}_0'''+\hat{F}_0''(1+\hat{F}_1'')+\hat{F}_0\hat{F}_1''-2\hat{F}_0'\hat{F}_1'=0,\\ \hat{G}_1'''+\xi\hat{G}_0'''+\hat{G}_0''(1+\hat{F}_1)+\hat{F}_0\hat{G}_1''-\hat{F}_0'\hat{G}_1'+\hat{F}_1'\hat{G}_0'=0,\\ \hat{H}_{1-1}''+\xi\hat{H}_{1-0}''+\hat{H}_{1-0}'+\hat{F}_0\hat{H}_{1-1}'+\hat{F}_1\hat{H}_{1-0}'-\hat{F}_0'\hat{H}_{1-1}-\hat{F}_1'\hat{H}_{1-0}-\alpha_1\hat{H}_{1-1}+\beta_1\hat{H}_{2-1}=0,\\ \hat{H}_{2-1}''+\xi\hat{H}_{2-0}''+\hat{H}_{2-0}'+\hat{F}_0\hat{H}_{2-1}'+\hat{F}_1\hat{H}_{2-0}'-\hat{F}_0'\hat{H}_{2-1}-\hat{F}_1'\hat{H}_{2-0}-\alpha_1\hat{H}_{2-1}-\beta_1\hat{H}_{1-1}=0,\end{cases} \tag{44}$$

where the boundary conditions become:

$$\begin{aligned}\hat{F}_0(0)&=\frac{S}{\varepsilon},\quad \hat{F}_0'(0)=0,\quad \hat{F}_0'(\infty)=1,\\ \hat{G}_0(0)&=\hat{G}_0'(0)=0,\quad \hat{G}_0''(\infty)=1,\\ \hat{H}_{1-0}(0)&=\hat{H}_{1-0}(\infty)=\hat{H}_{2-0}(0)=\hat{H}_{2-0}(\infty)=0,\end{aligned} \tag{45}$$

$$\begin{aligned}\hat{F}_1(0)&=\hat{F}_1'(0)=\hat{F}_1'(\infty)=0,\\ \hat{G}_1(0)&=\hat{G}_1'(0)=\hat{G}_1''(\infty)=0,\\ \hat{H}_{1-1}(0)&=\hat{H}_{1-1}(\infty)=\hat{H}_{2-1}(0)=\hat{H}_{2-1}(\infty)=0.\end{aligned} \tag{46}$$

Even though numerical integration of (43) is still difficult, but it is much easier than the original system of BVPs.

6. SHEAR STRESSES

The axial shear stress is calculated from:

$$\tau_{rz}=\mu\left(\frac{\partial w}{\partial r}+\frac{\partial u}{\partial z}\right), \tag{47}$$

DOI: 10.1002/fld

In which μ is the fluid viscosity. Using relations (11) and (12) the shear stress in the form of semi-similar solutions at the cylinder surface is:

$$\tau_{rz}=\frac{4\mu\bar{k}}{a}zf''(1)+\bar{k}\mu\gamma g''(1)+2\bar{k}\mu H'(1,\tau). \tag{48}$$

Some numerical results are presented in the next section.

7. PRESENTATION OF RESULTS

In this section the results of self-similar and semi-similar solutions, surface shear stresses and streamlines are presented. Figures 2 and 3 present the functions f and g. In 2(a) the functions f, f' and f'' and in 2(e) the functions g, g', g'' are presented for $Re=10$ and $S=0$. In 2(b), the function f and the boundary layer thickness decrease as Re increases and in 2(f), there is the same behavior for the function g. In Figures 2(c), (d), 3(a) and (b), the variations of the functions

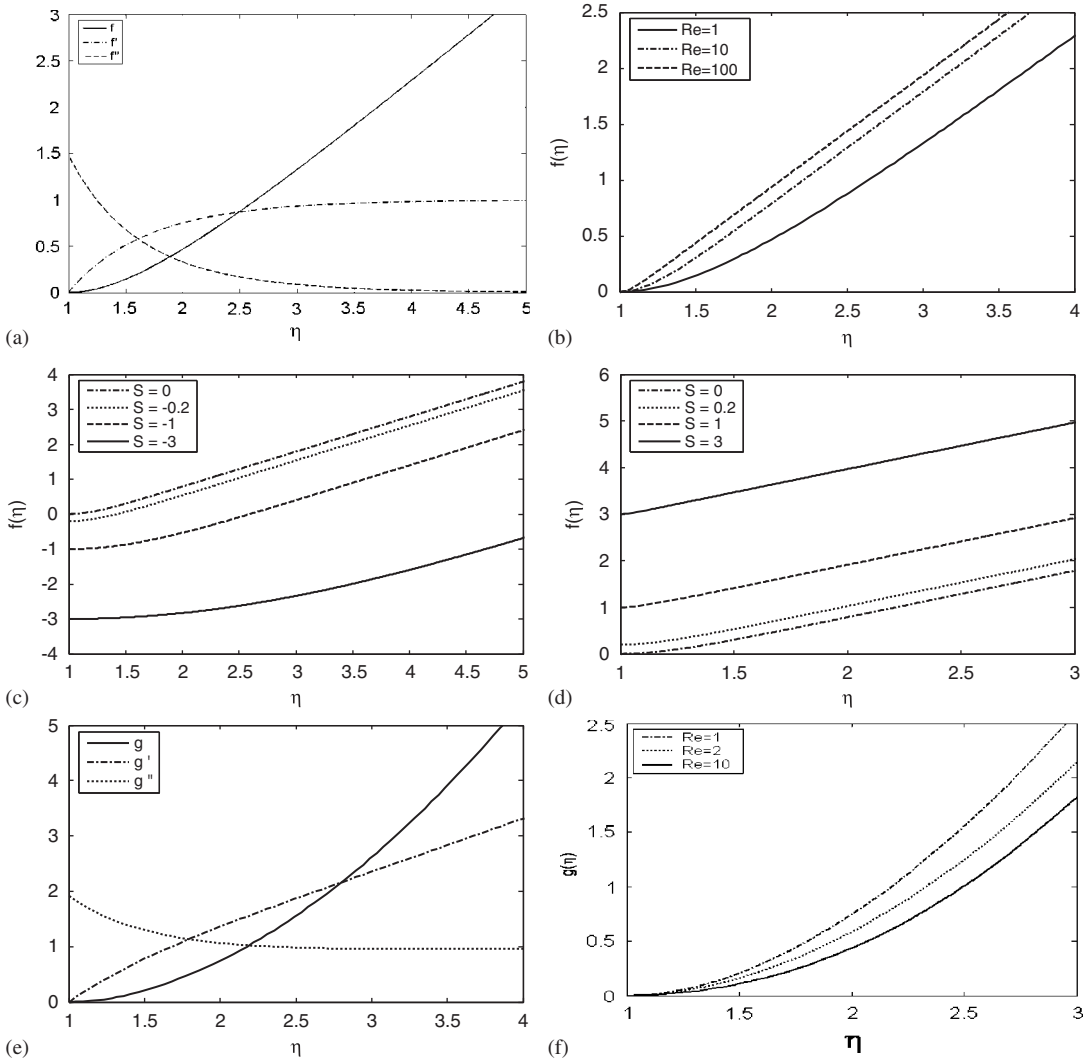

Figure 2. Sample profiles for f and g: (a) f, f' and f'' for $Re=1$ and $S=0$; (b) f for different Re and $S=0$; (c) f for different $S<0$ and $Re=10$; (d) f for different $S>0$ and $Re=10$; (e) g, g', g'' for $Re=1$ and $S=0$; and (f) g for different Re and $S=0$.

DOI: 10.1002/fld

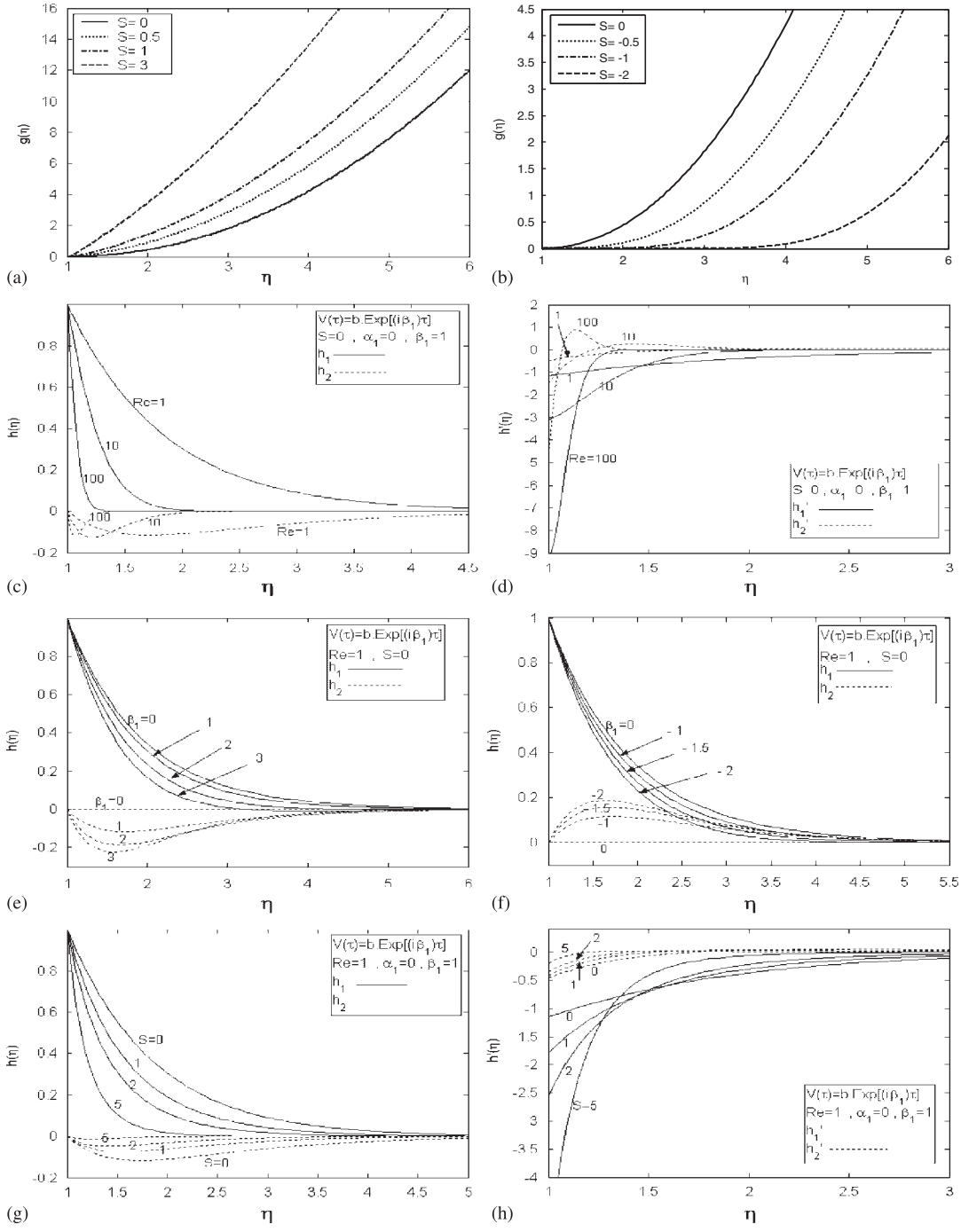

Figure 3. Sample profiles of g, h, h': (a) g for $Re=10$ and $S>0$; (b) g for $Re=10$ and $S<0$; (c) h and (d) h' for axial velocity $V(\tau)=b\cdot\mathrm{Exp}(\mathrm{i}\beta_1\tau)$ for different Re and $S=0$; (e) h for different $\beta_1>0$, $S=0$ and $Re=1$; (f) h for different $\beta_1\leqslant 0$, $S=0$ and $Re=1$; and (g) h and (h) h' for different suction rates and $Re=1$.

f and g for selected values of suction and blowing rate are shown. The more the suction value, the greater the function f will become at the cylinder surface.

For the sake of brevity, the self-similar results are presented only for $\alpha_1=1$ and $\beta_1=1$ (oscillating axial velocity). It is shown in Figure 3(c), (e)–(g) that increasing Re, β_1 and suction rate will result

DOI: 10.1002/fld

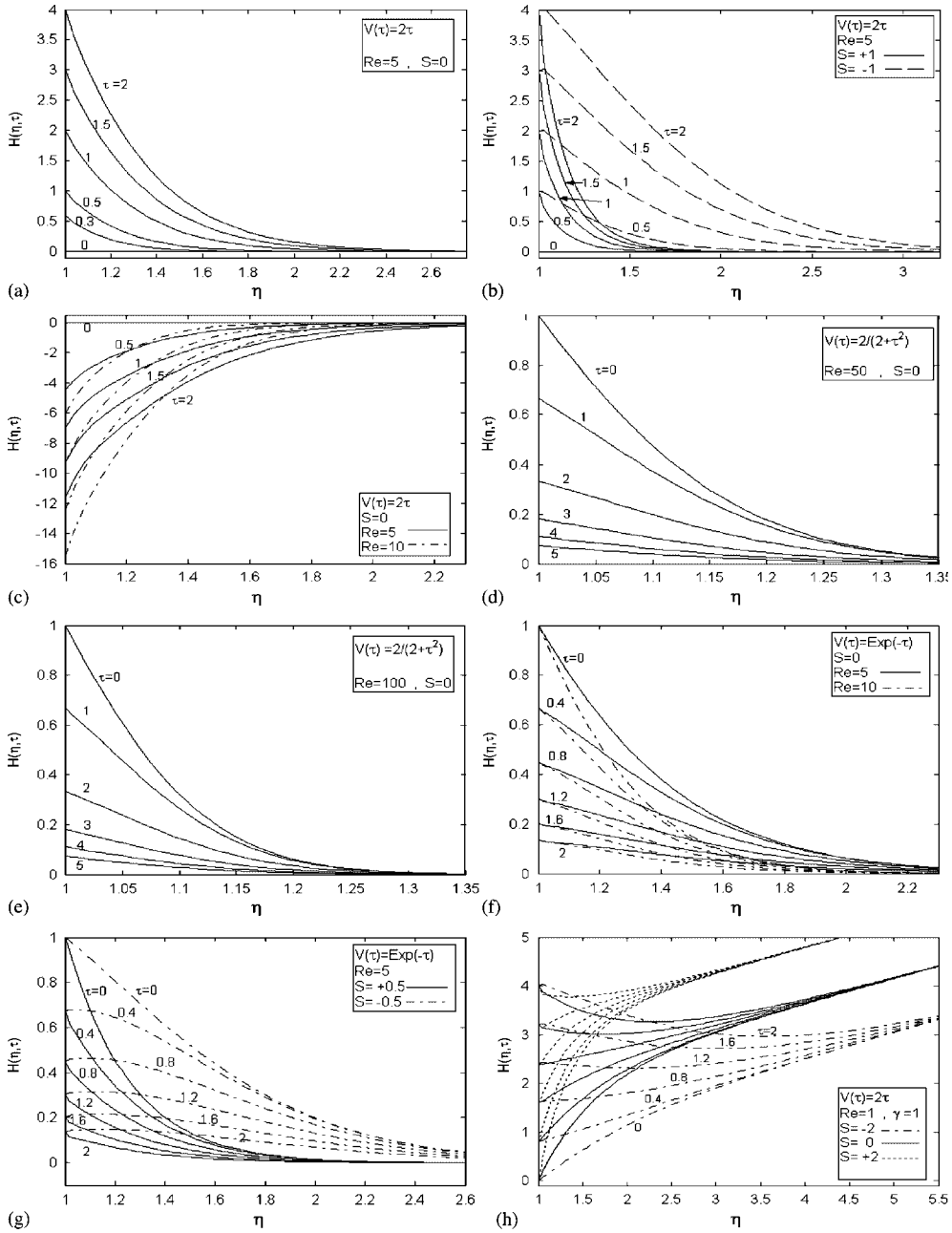

Figure 4. Sample profiles of H, H' and w: (a) H for axial velocity $V(\tau)=2\tau$ for $Re=5$ and $S=0$; (b) H for axial velocity $V(\tau)=2\tau$ for different suction rates and $Re=5$; (c) H' for axial velocity $V(\tau)=2\tau$ for different Re and $S=0$; (d) H for axial velocity $V(\tau)2/2+\tau^2$ for $Re=50$ and $S=0$; (e) H for axial velocity $V(\tau)2/2+\tau^2$ for $Re=100$ and $S=0$; (f) H for axial velocity $V(\tau)=\mathrm{Exp}(-\tau)$ for different Re and $S=0$; (g) H for axial velocity $V(\tau)=\mathrm{Exp}(-\tau)$ for different suction rates and $Re=5$; and (h) w for axial velocity $V(\tau)=2\tau$ for different suction rates and $Re=5$, $\gamma=1$.

in decreasing the function h, while blowing has an opposite effect. In Figure 3(d), and (h) different Re and S is presented for the function h'. Once again, increase in suction and Re values has a thinning effect in the boundary layer.

In Figure 4 semi-similar results of the function H are presented at different times for selected boundary conditions and different values of axial velocity.

DOI: 10.1002/fld

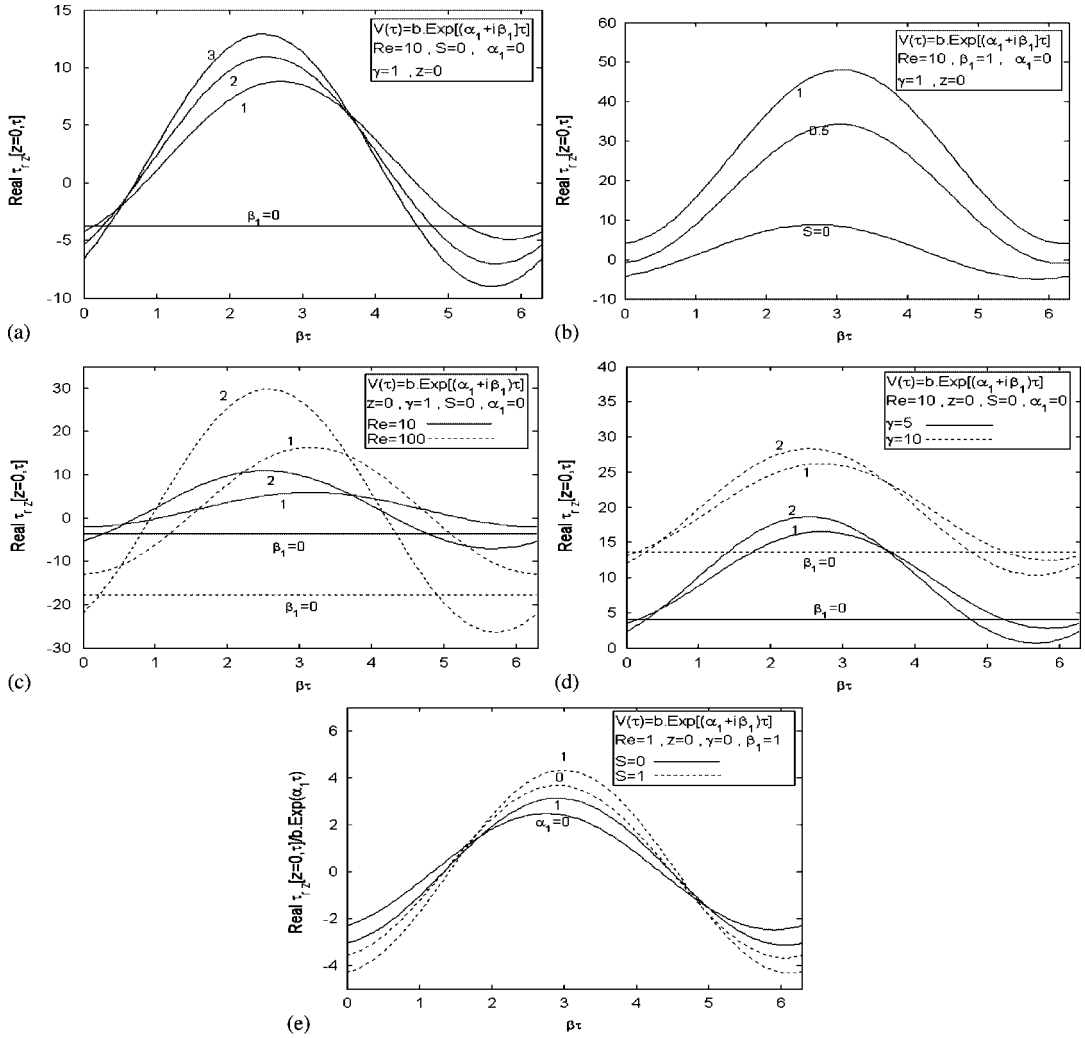

Figure 5. Axial shear stress at $\eta=1$, $z=0$ for cylinder with oscillating axial velocity $V(\tau)=b\cdot\mathrm{Exp}(\mathrm{i}\beta_1\tau)$ for (a) $Re=10$, $S=0$, $\gamma=1$ and different values of $\beta_1\geqslant 0$, (b) $Re=10$, $\beta_1=0$, $\gamma=1$ and different values of suctions, (c) $S=0$, $\gamma=1$ and different values of Re and β_1, (e) axial velocity $V(\tau)=b\cdot\mathrm{Exp}[(\alpha_1+\mathrm{i}\beta_1)\tau]$ and $Re=1$, $\beta_1=0$, $\gamma=0$ and different values of α_1 and S.

Axial shear stress τ_{rz} is presented at $\eta=1$, $z=0$ on the surface of the cylinder with harmonic and accelerating and oscillatory motion in Figure 5. In Figure 5(a) the maximum of the absolute value of shear stress becomes higher by increase of β_1. From Figure 5(b) it is evident that as the suction rate increases, the maximum of the absolute value of shear stress increases. Also in Figure 5(c) and (d), increase in γ and suction acts the same as increase in the absolute value of shear stress. In Figure 5(e), when the cylinder has an accelerating motion, the absolute value of shear stress becomes higher when the value of α_1 is increased.

Viscous stream function can be readily calculated according to similarity functions as:

$$\psi=\bar{k}a^2zf+\frac{\bar{k}a^3\gamma}{4}g+\frac{\bar{k}a^3}{2}\int_1^{\eta}H\,\mathrm{d}\zeta. \tag{49}$$

In Figure 6, the stream surface patterns of a cylinder with $v=0.5\tau$ are presented for selected values of flow parameters. The stagnation circle is not located at $z=0$, which is the outer inviscid stagnation circle location. We define z_s as the axial position of the viscous stagnation circle.

DOI: 10.1002/fld

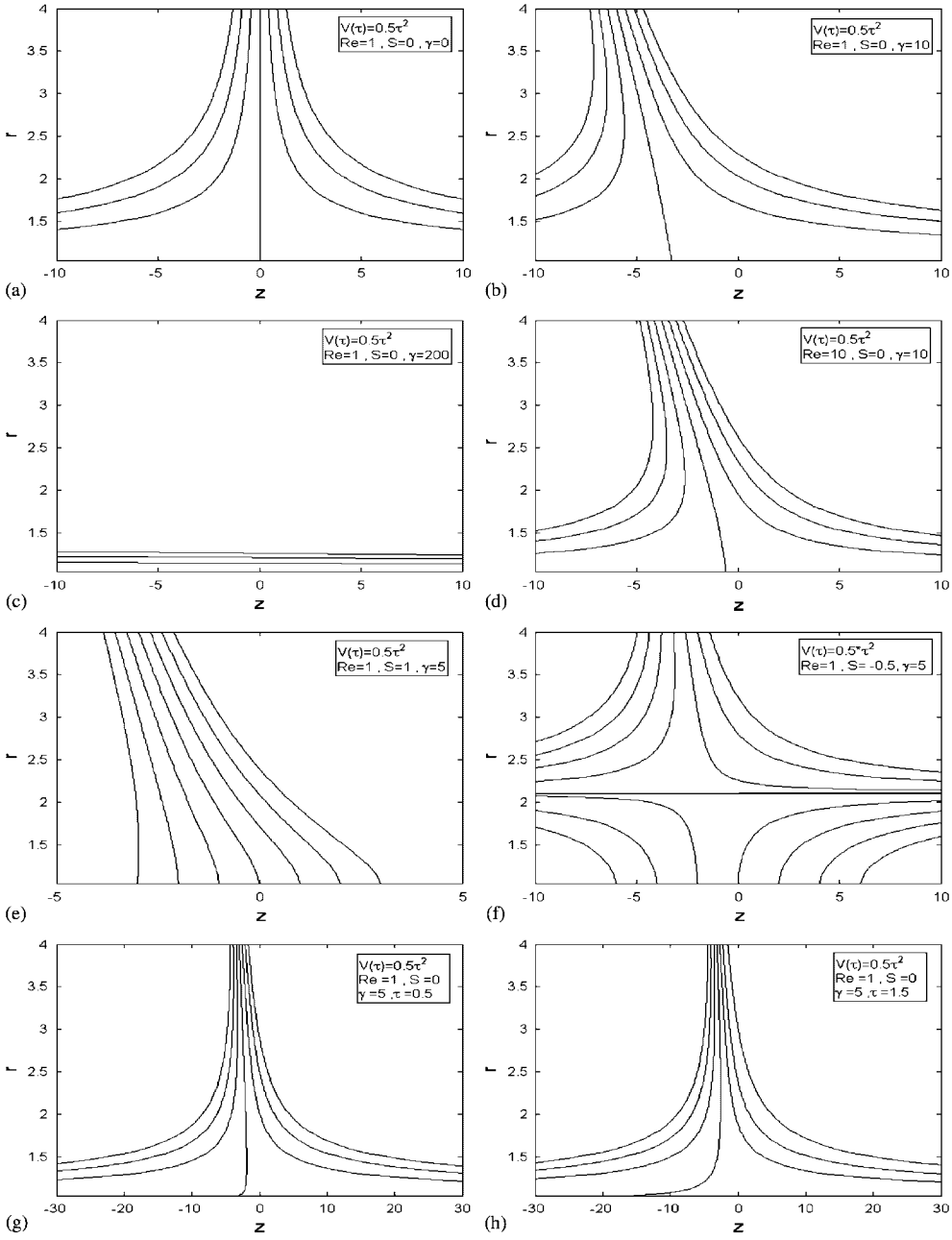

Figure 6. Stream surface patterns for $V(\tau)=0.5\tau^2$: (a) $\tau=0$, $Re=1$, $s=0$, $\gamma=0$; (b) $\tau=0$, $Re=1$, $s=0$, $\gamma=10$; (c) $\tau=0$, $Re=1$, $s=0$, $\gamma=200$; (d) $\tau=0$, $Re=10$, $s=0$, $\gamma=10$; (e) $\tau=0$, $Re=1$, $s=1$, $\gamma=5$; (f) $\tau=0$, $Re=1$, $s=-0.5$, $\gamma=5$; (g) $\tau=0.5$, $Re=1$, $s=0$, $\gamma=5$; and (h) $\tau=1.5$, $Re=1$, $s=0$, $\gamma=5$.

Mathematical expression for z_s is readily calculated, knowing the fact that the dividing stream surface $\psi=0$ intersects the cylinder at the axial position for which the axial shear stress is zero:

$$z_s=-\frac{a\gamma}{4}\frac{g''(1)}{f''(1)}-\frac{a}{2f''(1)}\left.\frac{\partial H}{\partial \eta}\right|_{\eta=1}. \tag{50}$$

As the value of γ increases with time, stagnation circle lies farther from the origin (see 6(a) and (b)) but increasing Re reduces it. In addition to reducing z_s, suction moves the stream surfaces into the cylinder and blowing moves them far away from it.

DOI: 10.1002/fld

8. CONCLUSIONS

An exact solution of the Navier–Stokes equations is obtained for the problem of stagnation-point flow on a moving circular cylinder with normal transpiration. In addition to the self-similar solution, which is obtained by separation of variables, the semi-similar solution is also carried out in order to analyze all different time-dependent axial movements.

Shear stresses will increase by increasing the values of γ, *Re* and suction rate, but they can be diminished by increasing the blowing rate. Finally, the deflection of the viscous stagnation circle from the free-stream stagnation circle is calculated and different parameters, such as suction rate, *Re*, γ and axial velocity on this deflection, is determined.

REFERENCES

1. Hiemenz K. Die grenzchicht an einem in den gleichformingen flus-sigkeitsstrom eingetauchten geraden kreiszylinder. *Dinglers Polytechnic Journal* 1911; **326**:321–410.
2. Homann FZ. Der einfluss grosser zahighkeit bei der strmung um den zylinder und um die kugel. *Zeitschrift für Angewandte Mathematik und Mechanik* 1936; **16**:153–164.
3. Howarth L. The boundary layer in three-dimensional flow part II. The flow near a stagnation point. *Philosophical Magazine* 1951; **42**:1433–1440.
4. Davey A. Boundary layer flow at a saddle point of attachment. *Journal of Fluid Mechanics* 1951; **10**:593–610.
5. Wang C. Axisymmetric stagnation flow on a cylinder. *Quarterly of Applied Mathematics* 1974; **32**:207–213.
6. Gorla RSR. Unsteady laminar axisymmetric stagnation flow over a circular cylinder. *Developments in Mechanics* 1977; **9**:286–288.
7. Gorla RSR. Nonsimilar axisymmetric stagnation flow on a moving cylinder. *International Journal of Engineering Science* 1978; **16**:392–400.
8. Gorla RSR. Transient response behavior of an axisymmetric stagnation flow on a circular cylinder due to time-dependent free stream velocity. *Letters in Applied Engineering Science* 1978; **16**:493–502.
9. Gorla RSR. Unsteady viscous flow in the vicinity of an axisymmetric stagnation-point on a cylinder. *International Journal of Engineering Science* 1979; **17**:87–93.
10. Gorla RSR. Heat transfer in an axisymmetric stagnation flow on a cylinder. *Applied Science Research* 1976; **32**:541–553.
11. Cunning GM, Davis AMJ, Weidman PD. Radial stagnation flow on a rotating cylinder with uniform transpiration. *Journal of Engineering Mathematics* 1998; **33**:113–128.
12. Takhar HS, Chamkha AJ, Nath G. Unsteady axisymmetric stagnation-point flow of a viscous fluid on a cylinder. *International Journal of Engineering Science* 1999; **37**:1943–1957.
13. Saleh R, Rahimi AB. Axisymmetric stagnation-point flow and heat transfer of a viscous fluid on a moving cylinder with time-dependent axial velocity and uniform transpiration. *Journal of Fluid Engineering* 2004; **126**:997–1005.
14. Rahimi AB, Saleh R. Axisymmetric stagnation-point flow and heat transfer of a viscous fluid on a rotating cylinder with time-dependent angular velocity and uniform transpiration. *Journal of Fluid Engineering* 2007; **129**:107–115.
15. Rahimi AB, Saleh R. Similarity solution of unaxisymmetric heat transfer in stagnation-point flow on a cylinder with simultaneous axial and rotational movements. *Transactions—American Society of Mechanical Engineers Journal of Heat Transfer* 2008; **130**:054502-1–054502-5.
16. Ziabakhsh Z, Domairry G, Ghazizadeh HR. Analytical solution of the stagnation-point flow in a porous medium by using the homotopy analysis method. *Journal of the Taiwan Institute of Chemical Engineers* 2009; **40**(1):91–97.
17. Weidman PD, Putkaradze V. Axisymmetric stagnation flow obliquely impinging on a circular cylinder. *European Journal of Engineering B. Fluids* 2003; **22**:121–131.
18. Press WH, Flannery BP, Teukolsky SA, Vetteling WT. *Numerical Recipes*, *the Art of Scientific Computing*. Cambridge University Press: Cambridge, 1997.

DOI: 10.1002/fld